2004

Microscale Distribution of Cesium Sorbed to Biotite and Muscovite

James Mckinley
Pacific Northwest National Laboratory, james.mckinley@pnl.gov

John M. Zachara
Pacific Northwest National Laboratory, john.zachara@pnl.gov

Steven Heald
Pacific Northwest National Laboratory

Alice Dohnalkova
Pacific Northwest National Laboratory

Matthew Newville
Argonne National Laboratory

See next page for additional authors

Environ. Sci. Technol. **2004**, *38,* 1017−1023

Microscale Distribution of Cesium Sorbed to Biotite and Muscovite

JAMES P. MCKINLEY,*,† JOHN M. ZACHARA,† STEVEN M. HEALD,†,‡ ALICE DOHNALKOVA,† MATTHEW G. NEWVILLE,§ AND STEVE R. SUTTON§

Pacific Northwest National Laboratory, Richland, Washington 99352, PNC-CAT and GSE-CARS, Argonne National Laboratory, Argonne, Illinois 60439

Individual 1−3 mm biotite and muscovite clasts from Hanford sediment were contacted with 0.08 M $CsNO_3$. They were examined using electron or X-ray microprobe methods, as intact specimens or sectioned perpendicular to their basal planes. Cs^+ was observed to preferentially sorb to mica edges, steps on mica surfaces, or fractured regions. The localization of Cs conformed to hypothesized strong binding to frayed edge sites in preference to sites on basal planes. In section, Cs^+ was found to penetrate the mica interior, forming discrete zones of concentration, particularly in muscovite. In biotite, Cs was more abundant, permeating the clasts, but also forming discrete zones of higher concentration. Concentrated Cs on both clast edges and within clast interiors corresponded to microscopic but relatively extensive zones where K was depleted. The localization of sorbed Cs in areas where K was depleted suggested that weathering reactions had caused the formation of frayed edge sites within the micas. Cs^+ accessed crystal interiors by diffusion along channels following crystal defects, cracks, or partings where pore fluids had previously migrated to form the interior alteration zones. On the nanometer scale, areas with localized Cs were disrupted, confirming that frayed edge sites were developed in clast interiors.

Introduction

Cesium-137 ($t_{1/2}$ = 30.17 y) is an important soil and vadose zone contaminant at the Hanford Site in southeastern Washington, which was active as a plutonium synthesis facility during the Manhattan Project and the Cold War. The chemical processing of fuel rods generated huge volumes of radioactive waste, some of which leaked from underground storage tanks or was disposed directly to the ground. About 4×10^{16} Bq (1 million Ci) of ^{137}Cs was leaked into the vadose zone, and sediment samples have been recorded to contain as much as 10^9 Bq g^{-1} (10^{10} pCi g^{-1}) ^{137}Cs. The site's micaceous sediment shows a high affinity for Cs^+, but cases of expedited Cs^+ migration have been observed when high-level waste was the carrier.[1] The residence and retention of ^{137}Cs in Hanford's unconsolidated sediments thus has significant consequences for deciding how and whether to remediate them.

Micaceous minerals present a favorable environment for Cs^+ adsorption.[2−6] They are common phyllosilicate minerals with a crystallographic sheet structure that consists of metal ions, principally aluminum and silicon, bound in octahedral and tetrahedral coordination, respectively, with oxygen.[7] Each sheet includes a central octahedral layer between two tetrahedral layers (Figure 1). Cations of lesser charge may substitute isomorphically for aluminum and silicon, imposing a net negative structural charge. Sheets are bound together by charge-compensating interlaminar K^+, which is weakly hydrated and fits into the mated ditrigonal cavities on the surfaces of adjacent sheets. The monovalent cations Cs^+ and Rb^+ are also weakly hydrated and similar in size to K^+, and so are strongly retained when substituted for K^+.

The importance of micaceous minerals for sorbing and retaining Cs has long been recognized. In addition to interrelated studies conducted by our group,[8−12] the retention of Cs^+ by micas has been intensively studied by others.[2−6,13−20] Much of this work, using contaminated sediments, mineral separates, or representative specimen minerals, was done to understand the behavior of anthropogenic Cs at sites that were contaminated in ways similar to the sediment at Hanford. The overall set of observations from the earlier work formed a relatively uniform framework for understanding and modeling Cs^+ interaction with micaceous minerals. In summary, the observations were (i) sorption occurred at two rates, a rapid initial sorption step followed by continued slow sorption during prolonged contact with the sorbing phase, (ii) desorption also proceeded at two rates, with rapidly and slowly desorbing fractions, (iii) when the adsorption event was prolonged, the slowly desorbing Cs^+ pool was a larger fraction of the whole, and (iv) in sediments where Cs^+ had a long residence, a significant fraction of adsorbed Cs^+ was resistant to desorption involving exposure to competing cations of varying relative selectivity and concentration.

The binding sites thought to explain these observations[5] (Figure 1) include (i) exchange sites on phyllosilicate surfaces, i.e., the accessible edge and basal plane sites, (ii) selective frayed edge site (FES) formed by the removal of K^+ from mica interlayers during natural weathering, and (iii) interlayer sites populated by the diffusion and displacement of K^+ by Cs^+ from FES. The wedge-shaped FES occupy the transition from an interlayer spacing of 1.4 nm at the weathered edge (where K^+ ions have been removed), to a spacing of 1.0 nm in internal unweathered interlayer space. Since they occupy a small fractional area on the mica surface, the abundance of FES is relatively small. The FES transition zone provides a favorable environment for binding weakly hydrated cations, such as K^+, Cs^+, and NH_4^+, which may readily displace weakly held, more strongly hydrated cations such as Na^+. Two-step adsorption could thus be explained by the rapid occupation of abundant low-affinity sites, followed by a fractional increase of occupancy in sparse high-affinity FES. The desorption-resistant Cs^+ could occupy interlayer sites or could represent Cs^+ trapped by interlayer collapse.

Recent studies focusing on ^{137}Cs at Hanford supplemented and improved the understanding of Cs^+ migration and retardation in micaceous sediments. In these sediments, ^{137}Cs was controlled by sorption to biotite and muscovite, with no other significant sorbing phases identified after exhaustive characterization of waste-impacted sediments using scanning electron microscopy and autoradiography.[12] Experimental investigations showed that the interaction of Cs^+ with these

* Corresponding author address: Pacific Northwest National Laboratory, MSIN K8-96, P.O. Box 999, Richland, WA 99352; phone: (509) 376-6573; fax: (509) 376-3650; e-mail: james.mckinley@pnl.gov.
† Pacific Northwest National Laboratory.
‡ PNC-CAT, Argonne National Laboratory.
§ GSE-CARS, Argonne National Laboratory.

10.1021/es034569m CCC: $27.50
Published on Web 01/14/2004

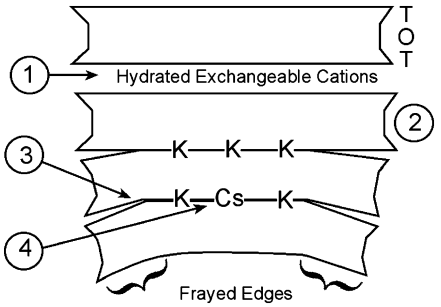

FIGURE 1. Schematic diagram of the mica structure: TOT, tetrahedral−octahedral−tetrahedral sheet structure; K and Cs, interlayer cations; edges are "frayed" by the removal of interlayer K^+. Potential sites for Cs^+ sorption: (1) cation exchange sites on the basal plane, (2) edge sites, (3) frayed edge sites, (4) replacement of K^+ by Cs^+ in interlayer sites.

sediments could be described using a four-parameter model with high- and low-affinity sites, including the effects of weakly interacting smectites;[10,11] the low-affinity component became more significant at relatively high fractional surface loadings. Desorption from contaminated sediments was controlled by a complex interaction of processes and included rapidly reversible and nonreversible components.[8] The desorption rate was dependent on electrolyte concentration, electolyte cation, and temperature.[21] The contaminated sediments were observed to have been significantly altered by interaction with highly alkaline wastes, with only 40% of the total Cs^+ measured to be exchangeable. In laboratory studies using contaminated sediments, the extent and rate of Cs^+ desorption were modeled to be influenced by surface armoring, intraparticle diffusion, and the collapse of edge-interlayer sites in the presence of K^+, Cs^+, or Rb^+. In applying laboratory measurements of Cs^+ sorption to the field, however, using sorption constants obtained from composited uncontaminated sediments, the two-site model successfully simulated the subsurface distribution of Cs^+ at Hanford.[10,21]

The conceptual model represented by earlier experimental observations was thus used to construct numerical models that could simulate the laboratory and field behavior of Cs^+. In large part, these simulations relied on an understanding of the mineralogy of the micaceous minerals, including their chemical weathering mechanisms. However, there was no effort to confirm the distribution of sorbed Cs^+ on and within mica clasts by observation. In addition, there were some inconsistencies between theoretical and conceptual considerations of Cs^+ binding that could possibly be clarified by observations of Cs^+ on mica surfaces. For example, very slow desorption from some micaceous sediments[3,13,22] could be due to distribution of Cs^+ in areas that were relatively inaccessible to desorbing cations. We thought that demonstrating the association of Cs^+ with specific chemical regimes on the mica surface could bring some new and relevant information for understanding its behavior in the environment. In this investigation, we applied electron microprobe (EMP), scanning electron microscopy (SEM), transmission electron microscopy (TEM), and X-ray microprobe (XMP) methods to examine the spatial distribution of Cs^+, K^+, and other ions in micas that had been contacted with $CsNO_3$ solutions in the laboratory.

Methods

Micas were hand-picked from Hanford formation sediments retrieved from a vadose zone borehole proximate to the S-SX Tank Farm at the Hanford Site in south central Washington state. The Hanford formation is comprised of Pleistocene catastrophic flood deposits from glacial Lake Missoula. The phyllosilicate and associated mineralogy have been described elsewhere.[11] The micas were segregated into dark biotite and colorless muscovite species on the basis of appearance (a small fraction of mica clasts were sheathed in vermiculitic alteration and were not studied). The mica clasts described here were placed in contact with 20 mL of an aqueous solution of $CsNO_3$ (0.08 M), in small batches of ca. 12 clasts of 1−3 mm diameter, for 14 or 28 days at room temperature, washed with deionized water, and air-dried. Mica surfaces were examined directly. The internal portions of individual clasts were examined by imbedding them in epoxy resin and making ca. 60 μm thick sections perpendicular to the basal planes. (Henceforth, for clarity, Cs^+ is used in discussing the potentially mobile ion, and Cs is used in reference Cs more generally and to measurements on the solid phase.)

For EMP analysis, elemental abundances were imaged by tuning each of three wavelength-dispersive spectrometers (WDS) to the X-ray emission lines for Fe, K, and Cs using standard materials. The JEOL 8600 was run with a 20 keV electron beam at a current of 20 nA under digital positional control. The X-rays were collected for 0.2 s for each element from each point in a 512 by 512 grid on the sample surface at a resolution determined by the magnification, typically yielding a 200−600 nm pixel size. Scanning electron photomicrographs were made using a JEOL 6340F scanning electron microscope at 10 keV and 10 nA beam current.

For TEM analysis, sections were examined using a JEOL 2010 high-resolution transmission electron microscope equipped with a LaB_6 filament operating at 200 kV. Material was embedded in acrylic resin, and blocks were sectioned to a 70 nm thickness on a microtome (Leica Ultracut UCT) to obtain cross sections of individual mica particles. Sections were mounted on 200 mesh copper grids coated with Formvar support film sputtered with carbon. Electron energy loss spectroscopy (EELS) was used for the detection and mapping of compositional information.

For XMP analysis, measurements were made at the Argonne National Laboratory Advanced Photon Source on either the Pacific Northwest Consortium Collaborative Access Team (PNC-CAT) beamline[23] or the GeoSoilEnviro Consortium for Advanced Radiation Sources (GSE-CARS) beamline. The samples were mounted to an open stepper motor-driven stage on an optical bench and moved relative to the X-ray beam, which was focused by Kirkpatrick−Baez mirrors to a diameter of 6 μm on the sample surface. Samples were tilted 30° from normal incidence in the horizontal to facilitate observation, and element-characteristic X-rays were detected with either a WDS or an energy-dispersive spectrometer (EDS). The X-ray flux was about 5×10^{11} photons s^{-1}. The beam energy was selected with a Si(111) double-crystal monochromator with an energy resolution of $\Delta E/E = 1.4 \times 10^{-4}$. For imaging, the incident energy was set to 7110 eV to only partially excite the Fe signal, avoiding detector saturation from high concentrations of Fe. The limit of detection was approximately 5×10^9 Cs atoms in the beam spot. Weight percent concentrations were not measured. Comparative results were obtained by observing the characteristic X-ray intensities for K and Cs across the area analyzed.

For each XMP image, intensities were mapped and assigned false colors using Noesys software (Fortner Research, Sterling, VA). Digital EMP, SEM, and XMP images were manipulated and merged using Photoshop (Adobe Systems).

Results and Discussion

Although the distribution of Cs on mica surfaces was variable within and between clasts, results for the 14- and 28-day exposures were the same within our ability to measure them. Micas that had not been exposed to $CsNO_3$ were analyzed by EMP and XMP methods and did not contain Cs detectable by either method (not shown).

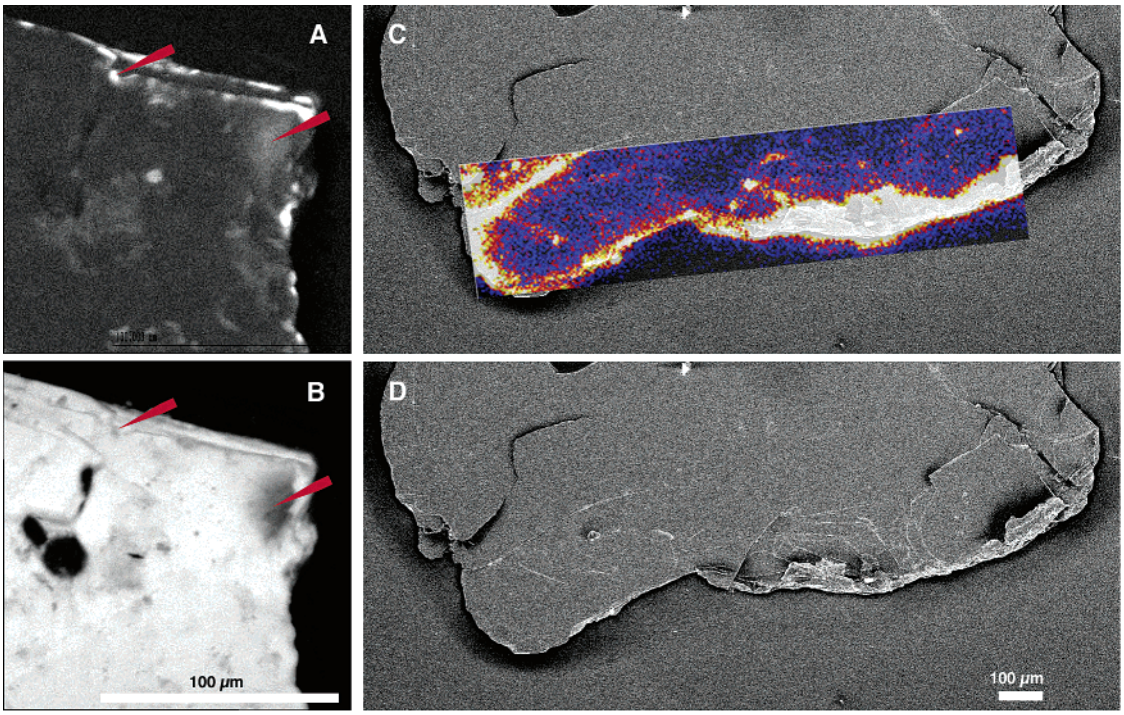

FIGURE 2. Cs on mica surfaces: left, Cs associated with biotite, elemental abundance map for Cs (A) and K (B); right, Cs associated with muscovite, superimposed secondary-electron SEM and false-color XMP image (C) and SEM image alone (D).

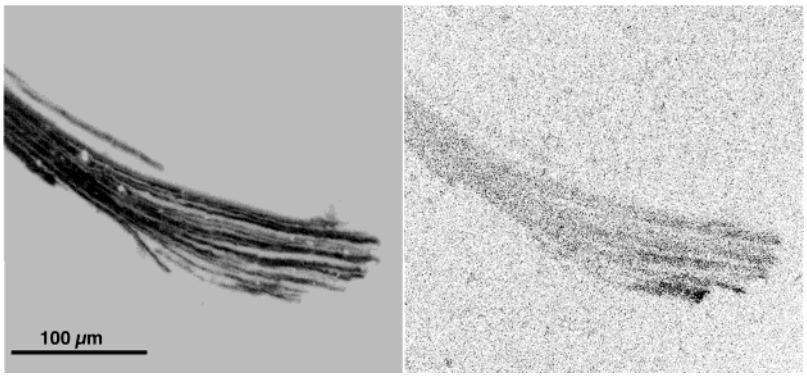

FIGURE 3. EMP elemental abundance maps for K (left) and Cs (right) on splayed muscovite. Darkness is proportional to concentration.

Clasts were imaged in terms of elemental abundances using XMP and EMP methods, and secondary electron or optical images were collected to provide a morphological reference for the compositional data. Since K was present in relatively high concentration (about 70−80 g kg^{-1} in muscovite and biotite[7]), abundance maps for K served to image clast morphology and provide data for comparison with Cs abundance. The results for mica surfaces (Figure 2) showed that Cs^+ was preferentially sorbed where individual sheet boundaries were expressed as steps on the clast surfaces. These steps were most abundant at, and of course defined, clast boundaries, so the Cs was most abundant on clast edges. Examination of the clast surface, particularly the surface of biotite, showed also that there were significant zones of K depletion and step edges not associated with clast boundaries (arrows, Figure 2A,B). It was apparent that K was depleted in areas with the most abundant Cs; this result was consistent with the formation of FES due to weathering reactions.

Muscovite sorbed less Cs^+ than biotite (using EMP analysis, Cs was readily detectible in biotite, but near the limit of detection in muscovite, e.g., Figures 2 and 3). Biotite is an Fe-rich trioctahedral mica (all sites in the octahedral sheet are occupied, and substitutions of divalent cations for Al^{3+} are common), whereas muscovite is dioctahedral (two-thirds of the octahedral sites are occupied by Al^{3+}, and the rest are vacant). The net negative structural charge in muscovite arises predominantly from Al^{3+} substitution for Si^{4+} in the tetrahedral sites, so that the charge deficiency is just adjacent to the interlayer space, and dioctahedral micas bind K^+ more strongly than trioctahedral micas.[24] Muscovite thus retains K^+ much more strongly than biotite. It is also the most weathering-resistant mica.[7,25] These mineralogical differences suggest that, under identical weathering conditions, muscovite could be expected to develop fewer Cs-complexing FES than biotite.

A sectioned muscovite (Figure 3) illustrated the cross sectional effects of chemical and physical weathering. The muscovite clast fanned as a result of exfoliation during weathering, with small domains of kaolinitization or primary mineral inclusions (light areas in the K image). In the EMP image, the depletion of K was not evident, and Cs was observed at low abundances, very near the limit of detection. The flayed lamina were observed at a size (2−10 μm) that was far larger than the weathering transition between 1.0 and 1.4 nm spacings, but their evident larger-scale alteration was a manifestation of alteration at a much finer scale. And, although Cs was near the limit of detection, it was obviously

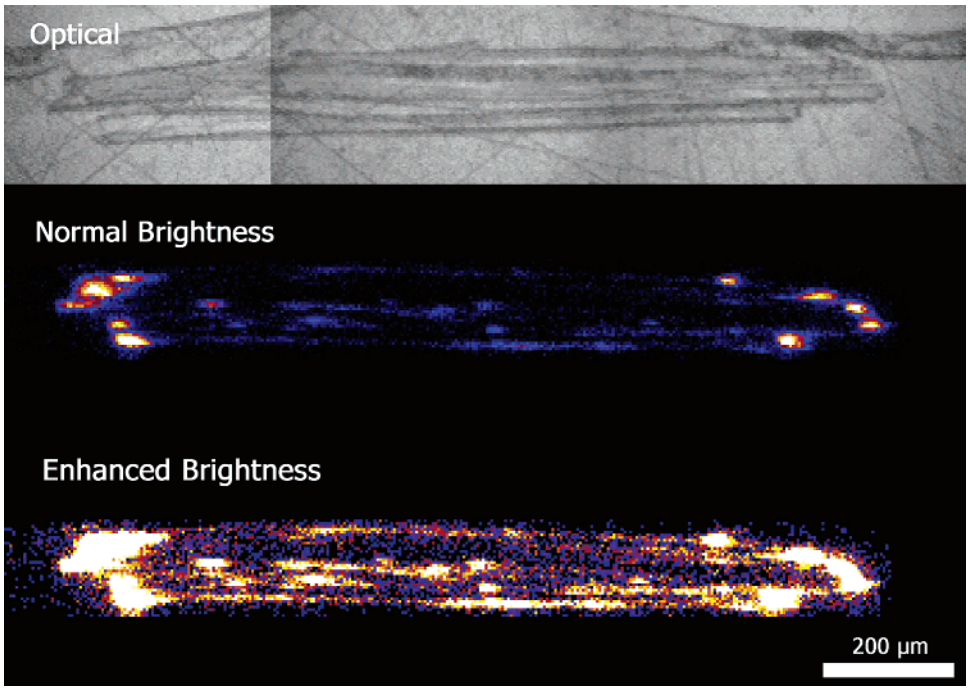

FIGURE 4. Optical image of sectioned muscovite clast with associated false-color Cs abundance. Cs is abundant at the clast ends (where FES were expected), and at the clast interior (where FES developed due to chemical weathering).

more abundant in the distal, delaminated regions of the muscovite clast.

The XMP provided more precise detail on the distribution of Cs in micas than the EMP. For muscovite (Figure 4) the data showed a striking heterogeneity in the distribution of Cs. Cs was concentrated near clast edges, as would be expected if the intensity of mechanical and chemical weathering, and the formation of FES, were greatest at the edges. Cs was not limited to edges, however, nor was it uniformly distributed, but was concentrated in discrete zones 3−6 μm across at clast edges and in the particle interior. The clustered near-edge Cs may indicate differential weathering and the development of zones of relatively abundant FES; however, the movement of Cs into the interiors of mica books by means other than diffusion along interlayer space has not been predicted or previously investigated.[5] The image in Figure 4 was a two-dimensional slice of a three-dimensional mineral clast, and we were aware of the possibility that the results were a two-dimensional expression of a process occurring in three dimensions. However, the deep penetration of Cs into the mica grain interiors argued against the interlayer diffusional replacement of K^+ by Cs^+: the distances traveled were too great.

Experimental studies of the potential rate of Cs^+ diffusion and replacement of K^+ in interlayer space indicate that it is extremely slow.[4] In an analogous study, early work with Rb^+ sorbed to micas also indicated limited migration of this Cs^+-like cation into interlaminar space.[25] In that study, micas were harshly treated to extract K^+ and then saturated with Mg^{2+}, after which Rb^+ was allowed to exchange with Mg^+ and residual K^+ in the induced FES. Rb was found on the solid only in the vicinity of steps and partings, and its relation to Mg^+ suggested that the Rb^+ induced the collapse of FES, causing its mobility to be self-limiting. This early observation was consistent with recent experimental evidence suggesting that excess K^+ could cause interlayer collapse and impede Cs^+ desorption.[8] A more likely explanation for the results in Figure 4 was the migration of Cs^+ along microfractures, cleavage partings, and crystallographic dislocations within the mica clasts to intragrain areas where FES were relatively abundant. Studies of mica weathering suggested that mica interiors were accessible to weathering solutions and reactions. The formation of vermiculite during the weathering of biotite, for example, was observed to include the formation of etch pits parallel to mica sheets, enclosing secondary noncrystalline and poorly crystalline clays.[26] These pits, occurring sporadically within mica clasts, were interpreted to be the result of dissolution at preexisting points of weakness, suggesting that the aqueous phase could access clast interiors. Weathering could thus have generated concentrated zones of FES in mica interiors, and the channels responsible for FES formation could act as conduits for Cs^+ diffusion.

In previous studies,[2−5,13,14] FES were typically and logically thought to be situated along the weathered edges of mica clasts. This approach was supported by correlations of sorption capacity and Cs^+ Kd to geometric surface area,[16] suggesting that FES were located on edges. The finding of FES in grain interiors as well as at edges is significant for the immobilization of $^{137}Cs^+$, since it implies that the effective surface area is larger than apparent, and could also explain the fractional migration of sorbed Cs^+ from "weak" to "strong" sites over time.

The sorption of Cs^+ was qualitatively different between biotite and muscovite. Biotite was extensively weathered, with abundant partings, fractures, and zones of K depletion (Figure 5). (In Figure 5, the brightness is proportional to the concentration of Fe and K, and to an increasing average atomic number for backscattered electron intensity, BSE.) Cs was generally detectable across the interiors of biotite clasts at relatively low abundance, with some areas having significantly higher concentrations (arrows in Figure 5). A comparison of morphology (BSE) with K abundance indicated areas of K depletion where the clast was physically intact. Cs tended to be concentrated in those areas. The retention of Cs^+ was thus apparently facilitated by weathering and the leaching of K^+ to produce abundant FES. Careful inspection of the distribution of Fe indicates also that Fe was more abundant in areas where Cs was concentrated (arrows). Increased Fe abundance at areas of relatively abundant Cs may have been due to Fe(II) oxidation and the resultant crystallographic changes and formation of FES. The micas

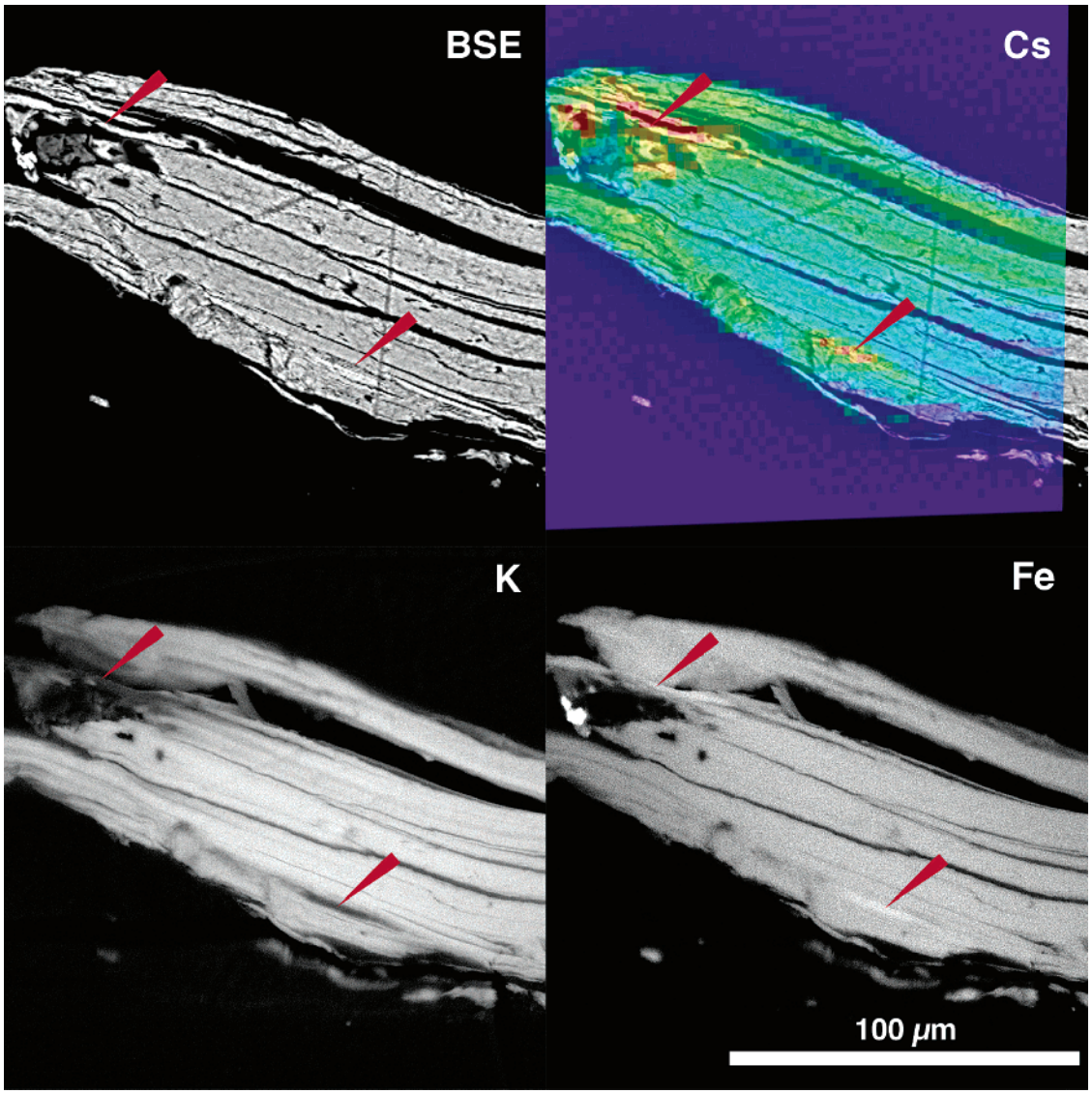

FIGURE 5. Morphology and elemental abundances for sectioned biotite clast. Arrows indicate concentrated Cs and Fe, and depleted K.

in Hanford sediments were transported and lay as individual clasts in an aerobic environment, and were documented to exhibit alteration aureoles indicative of Fe(II) oxidation.[11] More systematic studies of biotite weathering have also demonstrated the consequences of Fe(II) oxidation. In a study of biotite in a granitic weathering profile,[27] the oxidation of octahedral-layer Fe(II) was accompanied by the pervasive loss of K^+ and the expulsion of divalent octahedral cations to compensate the induced charge imbalance. The combination of Fe oxidation and cation loss caused delamination and the formation of secondary minerals, and mineral-structure discontinuities that acted as conduits for weathering solutions. This process may also have been extensive in the biotites in Hanford sediments. The localized increase in Fe abundance in Figure 5 probably resulted from the loss of Fe(II) from octahedral sites and the proximal precipitation of a ferric secondary mineral, as observed in studies where biotite was weathered experimentally.[28] An X-ray absorption near-edge structure (XANES) analysis of areas with maximum and minimum Cs (Figure 6) indicated a uniform distribution of Fe(III) throughout the clast; i.e., all structural Fe(II) was oxidized.

The evident mechanical damage from weathering and the observed compositional variations (Figure 5) suggested that Hanford biotites were pervasively altered by dissolution and the oxidation of Fe(II) to form abundant fluid-conducting

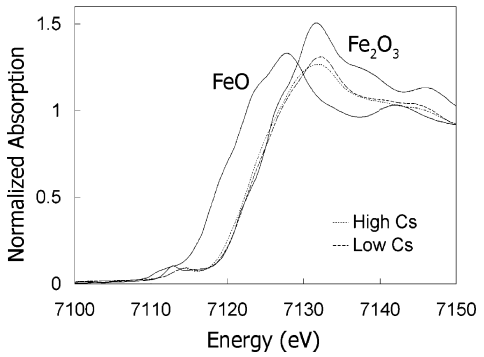

FIGURE 6. XANES spectra for high-Cs and low-Cs areas of Figure 5, compared to spectra for Fe(II) and Fe(III).

microchannels and K-depleted sites (FES) accessible by Cs^+. In contrast, the Hanford muscovites contained minor Fe (not quantified; muscovites generally include up to 20 g kg^{-1} FeO[7]). The development of internal zones of FES in muscovites may have been partially facilitated by Fe oxidation and leaching, although Fe(II) oxidation is not a prerequisite for dissolution and FES formation.[26]

Cesium sorption data published in 1972[29] included hypothetical mechanisms for the sorption and retention of

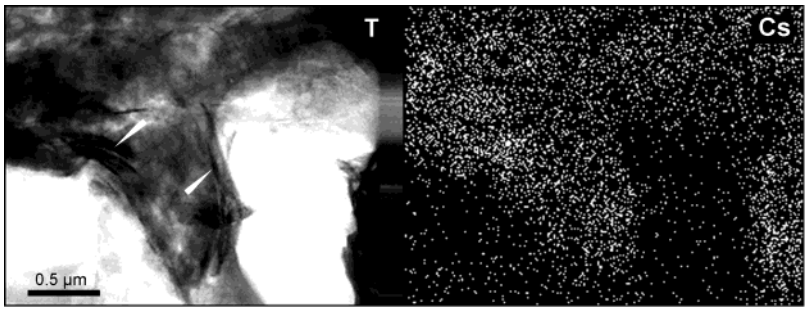

FIGURE 7. TEM image of muscovite with EELS abundance map for Cs.

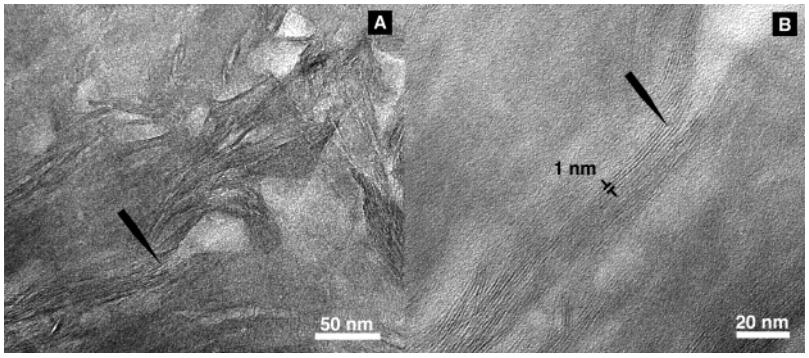

FIGURE 8. Detail of the Cs-rich area in muscovite. Lamina are parted and void spaces developed by chemical weathering (A). Parting (arrow denotes same area in parts A and B) forms wedge morphology (B).

weakly hydrated monovalent cations, including their selective retention in the transition zone where K had been removed from interlayer space (FES), and the collapse of expanded layers after binding these ions. Our data confirm directly the sorption of Cs^+ to sites at the edges of micas, on a microscopic level. The mineral chemistry of trioctahedral biotites and dioctahedral muscovites suggested that muscovite could have a greater affinity for Cs^+ than does biotite, as it does for K^+, and experimental investigations with these minerals indicated that this was so.[30,31] Our data and work with ^{137}Cs-contaminated sediment,[12] however, indicated that biotite retained much more Cs^+ in Hanford sediments than muscovite. The greater weathering of biotites in these sediments, to the extent that observable zones of K depletion were developed, suggested that biotite's relatively large concentration of FES could explain the higher retention of Cs^+.

The micrometer-scale observations of Cs concentration on mica surfaces and interiors suggested that Cs should be located in areas of observable chemical alteration on the nanometer scale. We tested this hypothesis by examining microtomed samples of muscovite using EELS to find areas of relatively abundant sorbed Cs^+. Areas where Cs was abundant were found to be pervasively altered (Figure 7). Dark, intact areas of mica sheets (arrows) were bent and discontinuous, and were surrounded by areas of disrupted sheets in chaotic arrangement. On a scale where mica sheet structures were distinguishable within the Cs-rich area (Figure 8A), the muscovite showed areas where sheet structures were crenellated, and areas of arcuate subparallel sheets defining voids that could represent weathered microchannels. On the nanometer scale in the same area (Figure 8B), the 1 nm muscovite basal spacing was preserved locally, but areas were also evident where sheets were parted to form FES-like structures. The residence of Cs^+ in micas where FES had formed was thus confirmed. These observations are consistent with the work of others who specifically investigated the effects of mica weathering, particularly the observed formation of partings and thin and curved packets of multiple sheet layers in weathered biotites.[27] The existence of FES in clast interiors, and not just near clast boundaries, may help to explain Cs^+ desorption behavior.

The diffusive migration of Cs^+ into dehydrated interlayer space in micas was previously hypothesized to explain its recalcitrance to desorption, although the estimation of very slow rates for this process suggests that it is unlikely to be significant.[4] Alternatively, the potential for monovalent cations to sorb to FES and cause the collapse of the mica structure[25,29] could explain slowly reversible sorption. A recent experimental and modeling study of $^{137}Cs^+$ desorption from sediments contaminated 30 years ago invoked this process.[8]

The broad distribution, shown here, of Cs within biotites, and the development of concentrated zones of Cs^+ accumulation within less weathered muscovites, suggests that pore fluids can access a significant intragrain region. Weathering-induced crystal defects, cracks, and partings within the mica structure may allow the diffusive access for dissolved ions and uninterrupted water saturation through capillary forces in the unsaturated vadose zone, allowing the redistribution of Cs^+ from low-affinity to high-affinity sites over time. Our experiments involved short-term exposure to dissolved Cs^+ (up to 28 days), and this contact time was sufficient to allow significant intragrain mass transport. The Cs^+ was then bound by FES within the mica. The inability of many investigators to desorb significant fractions of bound Cs^+ could thus be explained by the sorption of Cs^+ to unexpectedly abundant FES within grain interiors. The slowness of desorption from these sites could be exacerbated by the partial collapse of the mica structure around Cs^+ ions, delaying ready exchange with desorbing cations.

Acknowledgments

This research was supported by the U.S. Department of Energy Environmental Management Science Program. The PNC-CAT is supported by funding from the Basic Energy Sciences, U.S. Department of Energy, and by the Canadian Natural Sciences and Research Council. The TEM work was performed at the W. R. Wiley Environmental Molecular Sciences Laboratory, a national scientific user facility spon-

sored by the U.S. Department of Energy's Office of Biological and Environmental Research and located at Pacific Northwest National Laboratory (PNNL). PNNL is operated for the Department of Energy by Battelle. We thank four anonymous reviewers whose comments were very helpful.

Literature Cited

(1) Serne, R. J.; Zachara, J. M.; Burke, D. S. *Chemical Information on Tank Supernatants, Cs Adsorption From Tank Liquids Onto Hanford Sediments, and Field Observations of Cs Migration From Past Tank Leaks*; PNNL-11495; Pacific Northwest National Laboratory: Richland, WA, 1998.
(2) Francis, C. W.; Brinkley, F. S. *Nature* **1976**, *260*, 511−513.
(3) Evans, D. W.; Alberts, J. J.; Roy A., I. C. *Geochim. Cosmochim. Acta* **1983**, *47*, 1041−1049.
(4) Comans, R. N. J.; Haller, M.; de Preter, P. *Geochim. Cosmochim. Acta* **1991**, *55*, 433−440.
(5) Cornell, R. M. *J. Radioanal. Nucl. Chem.* **1993**, *171*, 483−500.
(6) Poinssot, C.; Baeyens, B.; Bradbury, M. H. *Geochim. Cosmochim. Acta* **1999**, *63*, 3217−3227.
(7) Deer, W. A.; Howie, R. A.; Zussman, J. *Rock-Forming Minerals, Volume 3. Sheet Silicates*; Longmans: London, 1976.
(8) Liu, C.; Zachara, J. M.; Smith, S. C.; McKinley, J. P.; Ainsworth, C. C. *Geochim. Cosmochim. Acta* **2003**, *67*, 2893−2912.
(9) Liu, C.; Zachara, J. M.; Qafoku, O.; Smith, S. C. *Environ. Sci. Technol.* **2003**, *37*, 2640−2645.
(10) Liu, C.; Zachara, J. M.; Smith, S. C. *J. Contam. Hydrol.*, in press.
(11) Zachara, J. M.; Smith, S. C.; Liu, C.; McKinley, J. P.; Serne, R. J.; Gassman, P. L. *Geochim. Cosmochim. Acta* **2002**, *66*, 193-211.
(12) McKinley, J. P.; Zeissler, C. J.; Zachara, J. M.; Serne, R. J.; Lindstrom, R. M.; Schaef, H. T.; Orr, R. D. *Environ. Sci. Technol.* **2001**, *35*, 3433−3441.
(13) Comans, R. N. J.; Hockley, D. E. *Geochim. Cosmochim. Acta* **1992**, *56*, 1157−1164.
(14) Sawhney, B. L. *Clays Clay Miner.* **1970**, *18*, 47−52.
(15) Grutter, A.; Gunten, H. R. v.; Kohler, M.; Rossler, E. *Radiochim. Acta* **1990**, *50*, 177−184.
(16) Rajec, P.; Sucha, V.; Eberl, D. D.; Srodon, J.; Elsass, F. *Clays Clay Miner.* **1999**, *47*, 755−760.
(17) De Preter, P.; Van Loon, L.; Maes, A.; Cremers, A. *Radiochim. Acta* **1991**, *52/53*, 299−302.
(18) Brouwer, E.; Baeyens, B.; Cremers, A. *J. Phys. Chem.* **1983**, *87*, 1213−1219.
(19) Liu, D.-C.; Hsu, C.-N.; Chuang, C.-L. *Appl. Radiat. Isot.* **1995**, *46*, 839−846.
(20) Klobe, W. D.; Gast, R. G. *Soil. Sci. Soc. Am. Proc.* **1970**, *34*, 746−750.
(21) Liu, C.; Zachara, J. M.; Qafoku, O.; Smith, S. C. Submitted for publication.
(22) Smith, J. T.; Comans, R. N. J. *Geochim. Cosmochim. Acta* **1996**, *60*, 995−1004.
(23) Heald, S. M.; Brewe, D. L.; Stern, E. A.; Kim, K. H.; Brown, F. C.; Jiang, D. T.; Crozier, E. D.; Gordon, R. A. *J. Synth. Radiat.* **1999**, *6*, 347−349.
(24) Jackson, M. L.; Sherman, G. D. *Adv. Agron.* **1953**, *5*, 219−318.
(25) Le Roux, J.; Rich, C. I.; Ribbe, P. H. *Clays Clay Miner.* **1970**, *18*, 333−338.
(26) Banfield, J. F.; Eggleton, R. A. *Clays Clay Miner.* **1988**, *36*, 47−60.
(27) Jeong, G. Y.; Kim, H. B. *Am. Mineral.* **2003**, *88*, 352−364.
(28) Murakami, T.; Utsinomiya, S.; Yokoyama, T.; Kasama, T. *Am. Mineral.* **2003**, *88*, 377−386.
(29) Sawhney, B. L. *Clays Clay Miner.* **1972**, *20*, 93−100.
(30) Dolcater, D. L.; Lotse, E. G.; Syers, J. K.; Jackson, M. L. *Soil. Sci. Soc. Am. Proc.* **1968**, *32*, 795−798.
(31) Torstenfelt, B.; Andersson, K.; Allard, B. *Chem. Geol.* **1982**, *36*, 123−137.

Received for review June 6, 2003. Revised manuscript received October 30, 2003. Accepted November 14, 2003.

ES034569M